Short communication

SURFACE and INTERFACE ANALYSIS

Received: 14 November 2012 Revised: 27 January 2013 Accepted: 30 January 2013 Published online in Wiley Online Library: 6 March 2013

(wileyonlinelibrary.com) DOI 10.1002/sia.5254

Investigating the morphology and mechanical properties of blastomeres with atomic force microscopy

Mi Li,[a,b] Changlin Zhang,[a,b] Liu Wang,[c] Lianqing Liu,[a]* Ning Xi,[a,d]* Yuechao Wang[a] and Zaili Dong[a]

Atomic force microscopy (AFM) was used to directly investigate the morphology and mechanical properties of blastomeres during the embryo development. With AFM imaging, the surface topography of blastomeres from two-cell, four-cell, and eight-cell stages was visualized, and the AFM images clearly revealed the blastomere's morphological changes during the different embryo developmental stages. The section measurements of the AFM topography images of the blastomeres showed that the axis of the embryos nearly kept constant during the two-cell, four-cell, and eight-cell stages. With AFM indenting, the mechanical properties of living blastomeres from several embryos were measured quantitatively under physiological conditions. The results of mechanical properties measurements indicated that the Young's modulus of the two blastomeres from two-cell embryo was different from each other, and the four blastomeres from the four-cell embryo also had variable Young's modulus. Besides, the blastomeres from two-cell embryos were significantly harder than blastomeres from four-cell embryos. These results can improve our understanding of the embryo development from the view of cell mechanics. Copyright © 2013 John Wiley & Sons, Ltd.

Keywords: atomic force microscopy; mechanical properties; Young's modulus; blastomere; embryo

Introduction

Forces are increasingly recognized as major regulators of cell structure and function, and the mechanical properties of cells play a critical role in the mechanisms of mechanotransduction by which the mechanical stimuli were converted into biochemical information.[1] The inherent mechanical properties of cells can ensure the progress of cellular physiological functions. Once the cell mechanical properties deviated from the normal level, the mechanotransduction then dysregulated, and this may induce human diseases.[2,3] Hence, investigating cellular mechanics is of great significance for unlocking the mystery of life. However, no analogous research on the relation between cell mechanical properties and human diseases took place until recently due to the advent of atomic force microscopy (AFM).[4] By controlling AFM tip to indent the sample, force curves can be obtained, and then the Young's modulus of the sample can be computed from the force curves.[5] Besides, AFM can work in liquids which are necessary for living cells, and these advantages makes AFM very suitable for characterizing the mechanical properties of living cells.[6] Many researchers have used AFM to investigate the cellular mechanical properties, and the results indicated that cell mechanical properties were a novel biomarker that can be used to represent the status of cells: cancer cells are softer than healthy cells,[7] and aggressive cancer cells are softer than indolent cancer cells.[8,9]

In the embryo development, blastomeres of the early mouse embryo are thought to be equivalent in their development properties at least until the eight-cell stage, but recent researches indicated that two-cell stage blastomeres have distinguishable fates in embryo development and four-cell stage mouse blastomeres have different developmental properties.[10–12] In view of the significance of cell mechanics, many researchers have investigated the mechanical properties of the developmental embryos, by using micropipette method [13] or AFM.[14] Sun *et al.* [13] have used a micropipette-based micro-robotic system to characterize the mechanical properties of mouse embryo zona pellucida (ZP), and the results revealed that the elastic modulus of embryos was 2.3 times larger than that of oocytes. Papi *et al.* [14] have used AFM to quantify the mechanical properties of three oocytes (immature, matured, and fertilized), and the results showed the first-decrease and then-increase trend of the elastic modulus of oocytes in the three stages. These researches have improved our understanding of the fertilized process from mechanical view, but these researches were performed on the ZP, not on the blastomeres inside ZP. Here, in order to investigate the mechanical properties of the blastomeres

* *Correspondence to: Lianqing Liu, Ning Xi, State Key Laboratory of Robotics, Shenyang Institute of Automation, Chinese Academy of Science, Shenyang 110016, China*
E-mail: lqliu@sia.cn; xin@egr.msu.edu

a *State Key Laboratory of Robotics, Shenyang Institute of Automation, Chinese Academy of Sciences, Shenyang 110016, China*

b *University of Chinese Academy of Sciences, Beijing 100049, China*

c *State Key Laboratory of Reproductive Biology, Institute of Zoology, Chinese Academy of Sciences, Beijing 100101, China*

d *Department of Mechanical and Biomedical Engineering, City University of Hong Kong, Hong Kong, China*

Copyright © 2013 John Wiley & Sons, Ltd.

in different embryo developmental stages, we used AFM to measure the mechanical properties directly on blastomeres in different mouse embryo developmental stages (two cell, four cell, and eight cell), and also the detailed topography of the blastomeres were visualized by AFM imaging.

Materials and methods

Sample preparation

Female mice were superovulated by intrapetritoneal injection of 7.5 IU of pregnant mares serum gondotrophin followed 48 h later by injection of 7.5 IU of human chorionic gonadotrophin, as described in reference.[10] Then, the female mice were mated with male mice. The fallopian tubes of the female mice were extracted, and then the fertilized eggs were picked from the fallopian tubes with the use of stereomicroscope. These fertilized eggs were then placed in a Petri dish containing mouse embryo medium (a layer of paraffin oil was coated on the medium to avoid the evaporation of the medium), and the Petri dish was put into a cell incubator (37 °C and 5% CO_2). In the cell incubator, the fertilized eggs developed to two-cell embryos, four-cell embryos, and eight-cell embryos. For the three developmental stages (two cell, four cell, and eight cell), embryos were picked out with the use of glass micropipette. Then, the ZP of the embryo was removed chemically, and blastomeres were imaged and measured by AFM. For imaging, living blastomeres were attached onto the poly-L-Lysine-coated glass slides and then fixed by 4% paraformaldehyde for 20 min. For mechanical properties measurements, living blastomeres were attached onto the poly-L-Lysine-coated Petri dish containing mouse culture medium.

AFM imaging and measurements

A Bioscope Catalyst AFM (Veeco company, Santa Barbara, CA, USA) was used in the experiments. The constant spring of the cantilever (MLCT, Veeco company, Santa Barbara, CA, USA) used here was 0.01 N/m calibrated by thermal noise method.[15] The shape of this tip was pyramidal. The blastomeres imaging experiments were performed in air at contact mode. The mechanical properties measurements were performed in mouse embryo culture. After putting the Petri dish onto the stage of the AFM, AFM probe was guided onto the surface of blastomeres by the inverted optical microscope (Nikon Ti, Japan) and then force curves were obtained. For each blastomere, about 50 force curves were obtained on five locations around the center of the blastomere. All force curves were obtained at the same loading rate (ramp rate is 1 Hz, ramp size is 3 μm).

For computing the Young's modulus, the Hertz model of cone tip was used (because the shape of the tip here was pyramidal):

$$F = \frac{2E\delta^2 \tan\theta}{\pi(1-\upsilon^2)} \quad (1)$$

In these relations, υ is the Poisson ratio of the sample (0.5), δ is the indentation depth, θ is the half-opening angle of the AFM tip, E is the Young's modulus, and F is the applied loading force. The force curves were processed by using the software package programmed by ourselves using Matlab. The process of computing the Young's modulus of one blastomere was as follows: (i) Converting the approach curve into the indentation curve according to the contact point in the approach curve (the contact point was decided visually); (ii) Applying the Matlab program to process the indentation curve; (iii)After computing the Young's modulus values from 50 force curves, Gaussian function was used to fit the values to produce the Young's modulus for the blastomere.

Results and discussion

Figure 1 shows the AFM morphological images of blastomeres in the two-cell, four-cell, and eight-cell stages of embryo development. Figure 1(A–C) were the AFM height images of the blastomeres in two-cell, four-cell, and eight-cell stages, respectively. Figure 1(D–F) were the corresponding section curves along the lines denoted in Fig. 1(A–C). From the AFM images, the shape changes of blastomeres during embryo development can be clearly discerned. After the fertilization of the ovum by sperm, the embryogenesis starts. The zygote cell then divides into two-cell embryo, four-cell embryo, eight-cell embryo, morula, blastocyst, etc. [16]. Figure 1A shows a forming two-cell embryo, that is, the zygote was dividing into two blastomeres. From the section curves of this forming two-cell embryo (Fig. 1D), we can

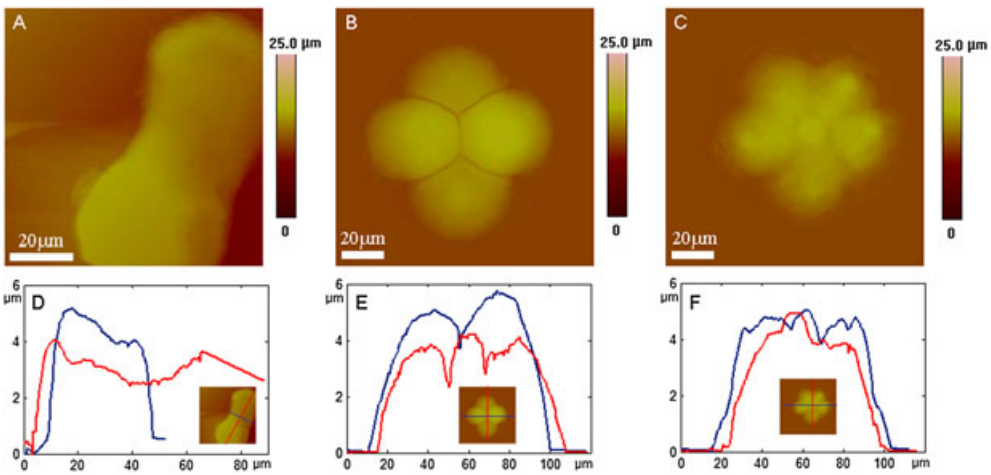

Figure 1. Imaging the topography of the blastomeres with AFM. AFM topography images of two-cell embryo (A), four-cell embryo (B), and eight-cell embryo (C). (D) Section curves of two-cell embryo. (E) Section curve of four-cell embryo. (F) Section curve of eight-cell embryo.

Copyright © 2013 John Wiley & Sons, Ltd.

see that the long axis of the embryo was about 90 μm, while the short axis of the embryo was about 40 μm. Figure 1B shows a four-cell embryo, that is, four blastomeres. The horizontal two blastomeres were next to each other, while the vertical two blastomeres were not next to each other. The section curves of this four-cell embryo (Fig. 1E) shows that the both of the horizontal axis and the vertical axis were about 90 μm. Figure 1C shows a forming eight-cell embryo, that is, the four-cell embryo was dividing into eight-cell embryo. From the AFM images, we can see that the shape of the forming eight-cell embryo is like plum blossom. From the section curves (Fig. 1F), we can see that the length of horizontal axis was similar to the length of vertical axis, and both of them were about 90 μm. Comparing the axis length of two-cell embryo, four-cell embryo, and eight-cell embryo, we can see that the axis nearly keeps the constant length (90 μm), this is because in the two-cell, four-cell, and eight-cell stages, the blastomers compact against each other and fill the zona pellucid.[17]

Figure 2 shows the mechanical properties measurement results of blastomeres during the embryo development. Under the guidance of the inverted optical microscope, AFM probe was moved onto the living blastomeres. The Petri dish was coated by poly-L-lysine which is positively charged, and then blastomeres were tightly adsorbed onto the Petri dish by electrostatic interactions. The Young's modulus of the blastomeres can be computed from the force curves by converting the force curves into indentation curves and then applying Hertz model.[7] Researches have shown that the loading rate of AFM tip influenced the measured Young's modulus.[3] Hence, we obtained all of the force curves at the same loading rate. Besides, considering that cells are heterogeneous, force curves were obtained on five locations around the central region of the cell. The process of computing cellular Young's modulus was shown in Fig. 2(A–C). Figure 2A was a typical force curve obtained on the blastomeres. The blue line corresponds to the approach curve, and the red line corresponds to the retract curve. The contact point in the approach curve can be easily discerned visually (the coordinate of the contact point was (2.266, −354.2). After converting the approach curve into the indentation curve according to the contact point, Hertz model was applied and often several hundred Young's modulus values can be computed from each indentation curve, as was shown in Fig. 2B. Gaussian fitting indicated that the Young's modulus was (2.32 ± 0.1) kPa. After putting the Young's modulus (2.32 kPa) into the Hertz model, the theoretical indentation curve was obtained (denoted by the red line in Fig. 2C), and we can see that the experimental indentation curve was consistent with the theoretical indentation curve.

For each blastomere, about 50 force curves were obtained, and these force curves were processed as the process depicted in Fig. 2(A–C). The measured Young's moduli of the blastomeres in two-cell and four-cell stages were shown in Fig. 2(D–E). First, the blastomeres from two two-cell embryos were measured, as shown in Fig. 2D. The Young's modulus of one blastomere from one embryo (denoted by the purple square in Fig. 2D) was (8.9 ± 0.75) kPa, and the Young's modulus of the other blastomere was (6.9 ± 1) kPa. The Young's modulus of one blastomere from the second embryo (denoted by the blue square in Fig. 2D) was (5.74 ± 1.62) kPa, and the Young's modulus of the other blastomere was (5.08 ± 1.89) kPa. We can see that the Young's modulus of the blastomers from the two-cell embryo was a little variable. Then, the blastomeres from two four-cell embryos were measured, as shown in Fig. 2E. The Young's modulus of the four blastomers from one embryo (denoted by the purple square in Fig. 2E) was (2.91 ± 0.76) kPa, (2.81 ± 0.38) kPa, (2.71 ± 0.23) kPa, and (1.84 ± 0.28) kPa, respectively. The Young's modulus of the four blastomers from the second embryo (denoted by the blue

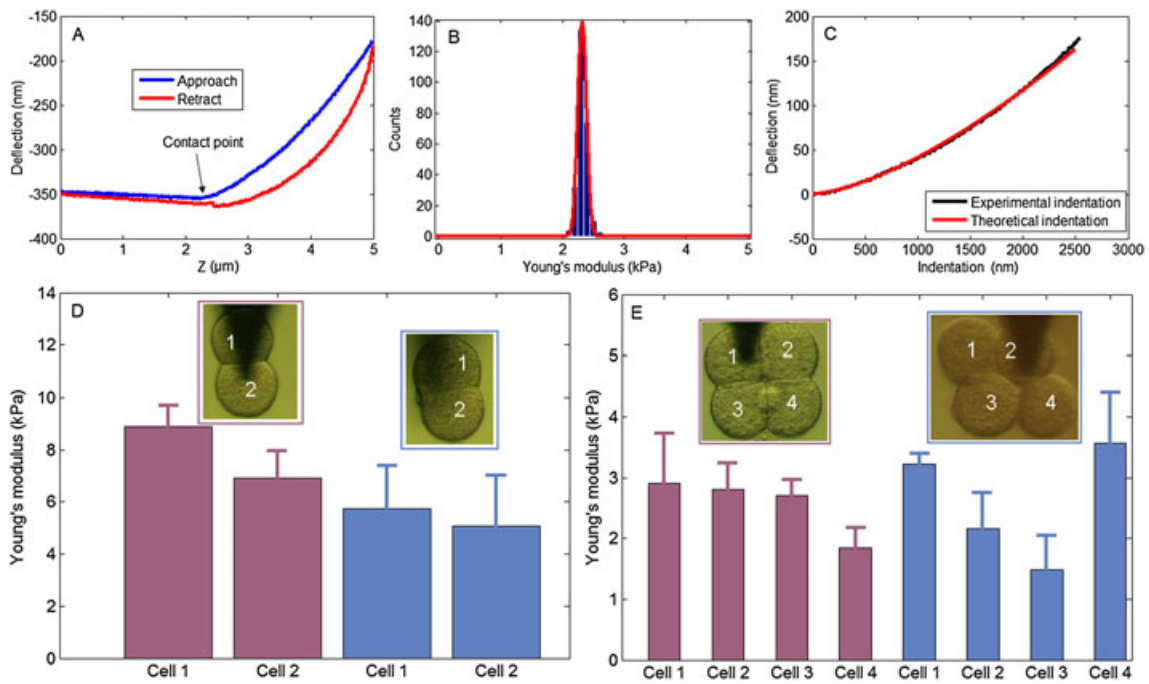

Figure 2. Measuring the mechanical properties of the blastomeres with AFM. (A) A typical force curve obtained on living blastomeres. The contact point in the approach curve was denoted by the arrow. (B) Histogram of the Young's modulus computed from the approach curve in (A). (C) Contrast of the experimental indentation curve (black line) and theoretical indentation curve (red line). (D) The measured Young's modulus of the blastomeres from two two-cell embryos. Insets are the optical images. (E) The measured Young's modulus of the blastomeres from two four-cell embryos. Insets are the optical images. (For interpretation of the references to color in this figure legend, the reader is referred to the web version of this article)

Copyright © 2013 John Wiley & Sons, Ltd.

square in Fig. 2E) was (3.22 ± 0.18) kPa, (2.16 ± 0.59) kPa, (1.48 ± 0.57) kPa, and (3.57 ± 0.79) kPa, respectively. Also we can see that the blastomeres from four-cell embryos had variable Young's modulus.

As shown in Fig. 2, the Young's modulus of blastomeres from two-cell stage was in the range of 4–10 kPa, while the Young's modulus of the blastomeres from four-cell stage was in the range of 1–4 kPa. From Fig. 1, we can see that the diameters of blastomeres from two-cell embryo are remarkably larger than that of the blastomeres from four-cell embryo. Besides, researches have shown that the expressions of microRNA were different in two-cell embryos and four-cell embryos.[18] These differences may cause that the mechanical properties of the blastomeres from two-cell stage were different from blastomeres from four-cell stage. The results also showed that the two blastomeres from two-cell stage had different Young's modulus, and the four blastomeres from four-cell stage had different Young's modulus. Researches have shown that since the first cleavage division of the mouse fertilized egg, the blastomeres had different fates [11]: the progeny of one blastomere primarily populate the embryonic part of the blastocyst and the progeny of the other blastomere populate the abembryonic part.[12] From these researches, we can see that blastomeres were different since the two-cell stage and this difference may cause the variable mechanical properties of the blastomeres during the two-cell and four-cell stages. The traditional methods for investigating the embryos are based on fluorescence labeling which might cause damage to cells.[19] Here, the experimental results showed that the blastomeres from different embryo developmental stages had variable Young's modulus, and if the cellular mechanical properties can be eventually related to the status of blastomeres in embryo development, then a label-free method can be established to investigate the behaviors of blastomeres in embryo development.

In summary, the morphology and mechanical properties of blastomeres during embryo development were investigated with the use of AFM. The morphology changes of blastomeres during the embryo developmental stages (two cell, four cell, eight cell) were directly visualized, and the AFM images showed that the axis length of the embryos nearly unchanged during the two-cell, four-cell, and eight-cell stages. By applying AFM indenting experiments, the mechanical properties of living blastomeres were measured quantitatively, and the results indicated that the Young's moduli of blastomeres were different with each other in both two-cell stage and four-cell stage.

Acknowledgements

This work was supported by the National Natural Science Foundation of China (61175103) and CAS FEA International Partnership Program for Creative Research Teams.

References

[1] P.A. Janmey, C.A. McCulloch, *Annu. Rev. Biomed. Eng.* **2007**, *9*, 1.
[2] A.W. Orr, B.P. Helmke, B.R. Blackman, M.A. Schwartz, *Dev. Cell* **2006**, *10*, 11.
[3] Q.S. Li, G.Y.H. Lee, C.N. Ong, C.T. Lim, *Biochem. Biophys. Res. Commun.* **2008**, *374*, 609.
[4] D. Kirmizis, S. Logothetidis, *Int. J. of Nanomed.* **2010**, *5*, 137.
[5] N.J. Tao, S.M. Lindsay, S. Lees, *Biophys. J.* **1992**, *63*, 1165.
[6] J.H. Hoh, C.A. Schoenenberger, *J. Cell Sci.* **1994**, *107*, 1105.
[7] S.E. Cross, Y.S. Jin, J. Rao, J.K. Gimzewski, *Nat. Nanotechnol.* **2007**, *2*, 780.
[8] W. Xu, R. Mezencev, B. Kim, L. Wang, J. McDonald, T. Sulchek, *PLoS One* **2012**, *7*, e46609.
[9] M. Li, L. Liu, N. Xi, Y. Wang, Z. Dong, X. Xiao, W. Zhang, *Sci. China Life Sci.* **2012**, *55*, 968.
[10] K. Piotrowska-Nitsche, A. Perea-Gomez, S. Haraguchi, M. Zernicha-Goetz, *Development* **2005**, *132*, 479.
[11] K. Piotrowska, F. Wianny, R.A. Pedersen, M. Zernicka-Goetz, *Development* **2001**, *128*, 3739.
[12] B. Plusa, A.K. Hadjantonakis, D. Gray, K. Piotrowska-Nitsche, A. Jedrusik, V.E. Papaioannou, D.M. Glover, M. Zernicka-Goetz, *Nature* **2005**, *434*, 391.
[13] Y. Sun, K.T. Wan, K.P. Roberts, J.C. Bischof, B.J. Nelson, *IEEE Trans. Nanobiosci.* **2003**, *2*, 279.
[14] M. Papi, R. Brunelli, G. Familiari, M.C. Frassanito, L. Lamberti, G. Maulucci, M. Monaci, C. Pappalettere, T. Parasassi, M. Relucenti, L. Sylla, F. Ursini, M.D. Spirito, *PLoS One* **2012**, *7*, e45696.
[15] J.L. Hutter, J. Bechhoefer, *Rev. Sci. Instrum.* **1993**, *64*, 1868.
[16] M. Zernicka-Goetz, *Nat. Rev. Mol. Cell Biol.* **2005**, *6*, 919.
[17] Y. Yamanaka, A. Ralston, R. O. Stephenson, J. Rossant, *Dev. Dyn.* **2006**, *235*, 2301.
[18] S. R. Viswanathan, C. H. Mermel, J. Lu, C.W. Lu, T. R. Golub, G. Q. Daley, *PLoS One* **2009**, *4*, e6143.
[19] X. Yu, D. Xu, Q. Cheng, *Preteomics* **2006**, *6*, 5493.

Copyright © 2013 John Wiley & Sons, Ltd.